European Journal of Pharmaceutics and Biopharmaceutics 70 (2008) 726–734

Contents lists available at ScienceDirect

European Journal of Pharmaceutics and Biopharmaceutics

journal homepage: www.elsevier.com/locate/ejpb

Research paper

Superior antitumor efficiency of cisplatin-loaded nanoparticles by intratumoral delivery with decreased tumor metabolism rate

Xiaolin Li [a,d], Rutian Li [e], Xiaoping Qian [a,e], Yitao Ding [a,e], Yunxia Tu [e], Rui Guo [b], Yong Hu [b], Xiqun Jiang [b], Wanhua Guo [c], Baorui Liu [a,e,*]

[a] Department of Oncology, Drum Tower Hospital Affiliated to Nanjing Medical University, Nanjing, 210008, PR China
[b] Laboratory of Mesoscopic Chemistry and Department of Polymer Science and Engineering, College of Chemistry and Chemical Engineering, Nanjing University, Nanjing, 210093, PR China
[c] Department of Nuclear Medicine, Affiliated Drum Tower Hospital, Medical School of Nanjing University, Nanjing, 210008, PR China
[d] State Key Laboratory of Pharmaceutical Biotechnology, Nanjing University, Nanjing, 210093, PR China
[e] Department of Oncology, Affiliated Drum Tower Hospital, Medical School of Nanjing University & Clinical Cancer Institute of Nanjing University, Nanjing, 210008, PR China

ARTICLE INFO

Article history:
Received 31 March 2008
Accepted in revised form 9 June 2008
Available online 26 June 2008

Keywords:
Nanoparticles
Drug delivery
Cisplatin
Antitumor
PET/CT

ABSTRACT

cis-Dichlorodiamminoplatinum (II) (cisplatin) has demonstrated extraordinary activities against a variety of solid tumors. However, the clinical efficacy is contrasted by its toxicity profile. To reduce the toxicity and enhance the circulation time of cisplatin, core–shell structure nanoparticles were prepared from block copolymer of methoxy poly(ethylene glycol)–polycaprolactone (mPEG–PCL). Cisplatin was incorporated into the nanoparticles with high encapsulation efficiency more than 75%. Controlled release of cisplatin was observed in a sustained manner. In vitro cytotoxicity studies proved the efficacy of cisplatin-loaded nanoparticles against BGC823 and H_{22} cells in a dose and time-dependent manner. Furthermore, intratumoral administration was applied to improve the tumor-targeted delivery in the in vivo evaluation. Compared with free cisplatin, cisplatin-loaded nanoparticles exhibited superior antitumor effect by delaying tumor growth when delivered intratumorally, while no significant improvement was observed when they were administrated intraperitoneally. Positron emission tomography/computed tomography (PET/CT) imaging was utilized for the first time to detect the declined ^{18}F-labeled 2-fluoro-2-deoxy-D-glucose (^{18}F-FDG) uptake of the tumor in mice receiving cisplatin-loaded nanoparticles intratumorally. These results suggest that polymeric nanoparticles with core–shell structures are promising for further studies as drug delivery carriers, and intratumoral delivery of drug-loaded nanoparticles could be a probable clinically useful therapeutic regimen.

© 2008 Elsevier B.V. All rights reserved.

1. Introduction

cis-Dichlorodiamminoplatinum (II) (cisplatin), one of the most widely used anticancer agents, has demonstrated extraordinary activities against a variety of solid tumors [1,2]. However, its therapeutic concentration is usually associated with dose-limiting side effects such as neurotoxicity, gastrointestinal disturbance, and especially nephrotoxicity [3]. In order to avoid the toxicity caused by the systemic administration (intravenous i.v., intraperitoneal i.p.) of cisplatin, nanoscale systems for cisplatin delivery have been designed on the basis of enhanced permeability retention (EPR) effect [4–6].

Two strategies are available to form cisplatin-loaded nanoparticles [4,6–11]. First, cisplatin is chemically conjugated with polymers to form a polymer–metal complex formation. Kataoka et al. firstly reported the conjugation between cisplatin and poly(ethylene glycol)–poly(aspartic acid) block copolymers [PEG–P(Asp)]. Further studies revealed the antitumor efficiency of the conjugates in tumor-bearing mice [7–9]. However, given that cisplatin in the state of conjugation showed no pharmacological effect, the actual antineoplastic efficacy of cisplatin–polymer conjugates primarily depends on the cisplatin released from the conjugates [9]. Consequently, the antitumor efficacy of cisplatin–polymer conjugates may be attenuated by the substantially slow release profile. Second, cisplatin is physically entrapped into the core–shell polymeric nanoparticles [4,6,10,11]. However, systemic administration (i.v., i.p.) failed to achieve high drug concentration in the tumor although it seems that antitumor effect was augmented in addition to the reduced side effects [12].

Locoregional chemotherapy emerges as an effective method to eradicate tumor. Intratumoral (i.t.) administration is adopted to extend the retention of drugs in the tumor tissue. Previous reports have demonstrated the ideally high drug concentration in tumors by i.t. delivery, but i.t. administration of free cisplatin failed to

* Corresponding author. Present address: Department of Oncology, Drum Tower Hospital Affiliated to Nanjing Medical University, Nanjing, 210008, PR. China. Tel./fax: +86 25 83107081.
E-mail address: baoruiliu@nju.edu.cn (B. Liu).

0939-6411/$ - see front matter © 2008 Elsevier B.V. All rights reserved.
doi:10.1016/j.ejpb.2008.06.016

achieve longer retention in the tumor because the low molecular weight of cisplatin resulted in rapid clearance and no significant improvement in antitumor efficacy was observed [13,14]. Compared to free cisplatin, cisplatin-loaded nanoparticles are characterized by the controlled release of incorporated cisplatin, which may overcome the deficiency of cisplatin retention in the tumor and may reach a satisfying outcome in improving antitumor efficacy when combined with intratumoral delivery. For instance, enhanced efficiency of paclitaxel or doxorubicin delivery systems by i.t. administration has been reported in earlier studies [12,15].

Treatment response measurements are essential in cancer therapy. In terms of the in vivo evaluation of antitumor efficacy, previous studies principally focused on the measurements of tumor volume. Actually tumor metabolism also is a vital phenomenon of cancer biology. Tumors with higher metabolism show increased uptake of glucose, which helps in localizing tumor and evaluating tumor activity. As a result, determination of tumor metabolism rate is of great significance in assessing the antitumor efficacy of chemotherapeutics. FDG–PET/CT has been shown to be a reliable predictor of treatment response in clinical practice. PET offers accurate metabolic images non-invasively, quantitatively and repeatedly. The innovative combination of PET and CT imaging provides precise fusion of PET images with high resolution anatomical CT images. PET–CT can image tumor metabolism, proliferation, hypoxia, and apoptosis with precise anatomic image fusion and will become an essential tool in the management of patients with cancer by its ability to assess disease extent, severity, and response to treatment. It has changed dramatically the management of numerous cancers. PET–CT will be used with increasing frequency and will become progressively used as a surrogate marker for disease response [16]. In this study, PET/CT was employed for the first time to evaluate tumor metabolism as measure of treatment response.

In this study, we prepared biodegradable core–shell mPEG–PCL nanoparticles incorporating cisplatin and examined the in vivo efficacy by i.t. and i.p. administration. Excellent biocompatibility of poly(epsilon-caprolactone) (PCL) lead to the US Food and Drug Administration approval and acceptance for medical applications. In addition, slow degradation of PCL based particles allow for extended release of the drug [17]. PEG possesses a number of outstanding physicochemical and biological properties. Because of its good biocompatibility, hydrophilicity, and the absence of antigenicity and immunogenicity, the core–shell structure with PEG as an outer shell enables the nanoparticles to escape from the scavenging of the reticuloendothelial systems (RES) in vivo effectively [18].

Moreover, PET/CT was utilized for the first time to investigate the metabolism rate of the transplanted tumor in different groups. This study demonstrated the superior antitumor efficacy of cisplatin-loaded nanoparticles compared to free cisplatin when they were delivered locally. PET/CT scanning also indicated the lower metabolism rate of the tumors in mice receiving cisplatin-loaded nanoparticles.

2. Materials and methods

2.1. Materials

Cisplatin was kindly provided by Jiangsu Hengrui Pharmceutical Co. Ltd. (Lianyungang, China). Methoxy-poly(ethylene glycol) (mPEG) (MW: 4, 10 kDa) was purchased from Sigma Chem. Co. (St. Louis, MO, USA). All PEG samples were dehydrated by azeotropic distillation with toluene, and then vacuum dried at 50 °C for 12 h before use. ε-Caprolactone (ε-CL, Sigma) was purified by drying over CaH_2 at room temperature and distillation under reduced pressure. Stannous octoate (Sigma) was used as received. All other chemicals were of analytical grade and used without further purification. Human gastric carcinoma cell line BGC823 and H_{22} cell lines were obtained from Shanghai Institute of Cell Biology (Shanghai, China).

Male ICR mice (6–8 weeks old and weighing 18–22 g) were purchased from Animal Center of Drum Tower Hospital (Nanjing, China).

2.2. Synthesis of mPEG and PCL block copolymers

mPEG–PCL block copolymers were synthesized by a ring opening copolymerization as previously described [19]. Briefly, predetermined amount of CL was added into a polymerization tube containing mPEG and a small amount of stannous octoate (0.1% wt/wt). The tube was then connected to a vacuum system, sealed off, and placed in an oil bath at 130 °C for 48 h. At the end of the polymerization, the crude copolymers were dissolved with dichloromethane (DCM) and precipitated into an excess amount of cold methanol to remove the un-reacted monomer and oligomer. The precipitates were then filtered and washed with water several times before thoroughly dried at reduced pressure. ^{1}H NMR and gel permeation chromatography (GPC) were utilized to characterize the copolymers.

2.3. Preparation of mPEG–PCL nanoparticles

Cisplatin-loaded nanoparticles were prepared by a nano-precipitation method as described previously with minor modification [19]. Briefly, 10 mg mPEG–PCL block copolymers and 0.6 mg cisplatin were dissolved in 0.5 ml dimethylformamide (DMF). The obtained organic solution was added dropwise into 5 ml distilled water under gentle stirring at room temperature. The solution was dialyzed to remove DMF thoroughly. The resulted bluish aqueous solution was filtered through a 0.45 μm filter membrane to remove non-incorporated drugs and copolymer aggregates. Since the analysis of quantitation on cisplatin loading efficiency showed good reproductivity for each batch, 20 batches were produced for the requirement of the in vivo experiments. Drug-free nanoparticles were produced in a similar manner without adding cisplatin. Solutions of cisplatin-loaded nanoparticles were then lyophilized for further characterization and utilization.

2.4. Characterization of nanoparticles

2.4.1. Size and zeta potential analysis of the nanoparticles

Mean diameter and size distribution were measured by photon correlation spectroscopy (DLS) with a Brookhaven BI-9000AT instrument (Brookhaven Instruments Corporation, NY, USA). Zeta potential was measured by the laser Doppler anemometry (Zeta Plus, Zeta Potential Analyzer, Brookhaven Instruments Corporation, NY, USA).

2.4.2. Transmission electron microscopy (TEM), atomic force microscopy (AFM)

Morphological examination of the nanoparticles was conducted with JEM-100S (Japan) transmission electron microscope (TEM). One drop of nanoparticle suspension was placed on a copper grid covered with nitrocellulose membrane and air-dried before negative staining with phosphotungstic sodium solution (1% wt/vol). Atomic force microscope (AFM) (SPI3800, Seiko Instruments, Japan) was used to study the surface morphology of nanoparticles in a greater detail. One drop of properly diluted nanoparticle suspension was placed on the surface of a clean silicon wafer and

dried under nitrogen flow at room temperature. The AFM observation was performed with a 20 μm scanner in a tapping mode.

2.4.3. Drug loading content (DLS) and encapsulation efficiency (EE)

Cisplatin loading content was determined by the $SnCl_2$ method with minor modification [8,20]. Briefly, lyophilized samples were dissolved in dimethylformamide (DMF) and 30 μl of this solution was mixed with 30 μl of 2 M HCL, followed by the addition of 2.94 ml of 0.2 M $SnCl_2$ solution in 2 M HCL. The absorbance of 403 nm was measured after 1 h with reference to a calibration curve on a Shimadzu UV-1205 Spectrophotometer (Kyoto, Japan). The following equations were applied to calculate the drug loading content and encapsulation efficiency.

Drug loading content (%) = weight of the drug in nanoparticles/weight of the nanoparticles × 100%.

Encapsulation efficiency (%) = weight of the drug in nanoparticles/initial amount of drug × 100%.

Nanoparticle yield (%) = weight of the nanoparticles/initial amount of polymers and drug × 100%.

2.5. In vitro release of cisplatin-loaded nanoparticles

The concentrations of unbounded cisplatin were determined using *o*-phenylenediamine as a ligand for cisplatin according to the method described by Kataoka et al. in Ref. [8]. Briefly, 1.2 ml of sample solution was mixed with an equal volume of 1.2 mg/ml *o*-phenylenediamine solution in DMF. The mixed samples were immerged into hot water bath (100 °C) for 10 min and the absorbance of 703 nm was measured immediately. Calibration was performed by standard cisplatin solution. For in vitro release detection, 10 mg lyophilized cisplatin-loaded nanoparticles were suspended in 1 ml of 0.1 M phosphate buffered saline (PBS, pH 7.4). The solution was then placed into a pre-swelled dialysis bag with a 12-kDa molecular weight cutoff and immersed into 20 ml 0.1 mol/l PBS, pH 7.4, at 37 °C with gentle agitation. One milliliters of samples was withdrawn from the incubation medium and measured for cisplatin concentration as described above. After sampling, equal volume of fresh PBS was immediately added into the incubation medium. The concentration of cisplatin released from the nanoparticles was expressed as a percentage of the total cisplatin in the nanoparticles and plotted as a function of time. Release study of free cisplatin was performed under the same condition.

2.6. In vitro cytotoxicity studies

Cytotoxicity of cisplatin-loaded nanoparticles against low differential human gastric cancer cell line BGC-823 and murine hepatic cancer cell line H_{22} was assessed by MTT assay, respectively [21]. Briefly, both cells were seeded in 96-well plates with a density around 5000 cells/well. BGC823 cells, not H_{22} cells, were allowed to adhere for 24 h prior to the assay. Then both cells were exposed to a series of doses of free cisplatin, empty nanoparticles, or cisplatin-loaded nanoparticles alone at 37 °C. After a predetermined times of incubation (24–72 h for BGC-823 cells, 48 h for H_{22} cells), 50 μl of MTT indicator dye (5 mg/ml in PBS, pH 7.4) was added to each well and the cells were incubated for another 2 h at 37 °C in the dark. The medium was withdrawn and 200 μl acidified isopropanol (0.33 ml HCl in 100 ml isopropanol) was added in each well and agitated thoroughly to dissolve the formazan crystals. The solution was transferred to 96-well plates and immediately read on a microplate reader (Bio-Rad, Hercules, CA, USA). Absorption was measured at a wavelength of 490 nm with 620 nm as a reference wavelength and obtained values were expressed as a percentage of the control cells to which no drugs were added. All experiments were repeated three times.

2.7. In vivo antitumor efficacy

ICR mice implanted with murine hepatoma cell line H_{22} were used to qualify the relative efficacy of cisplatin-loaded nanoparticles through two routes of administration (i.t., i.p.). The mice were raised under specific pathogen-free (SPF) circumstances and all the animal experiments were performed in full compliance with guidelines approved by the Animal Care Committee at Drum Tower Hospital. ICR mice were subcutaneously injected at the left axillary space with 0.1 ml of cell suspension containing 4–6 × 10^6 H_{22} cells. Treatments were started after 7–8 days of implantation. The mice whose tumor reached a tumor volume of 100 mm^3 were selected, and this day was designated as "Day 0".

For i.t. injections, animals received a single injection volume of ~0.2 ml with a 21-gauge needle placed in the center of the tumor. The i.t. injections were infused about 10 s, and the needle was allowed to remain in place for an additional 10–15 s and removed through another direction. On Day 0, the mice were randomly divided into eight groups, with each group being composed of 6 mice. The mice were treated i.t. with free cisplatin, cisplatin nanoparticles, empty nanoparticles and saline, respectively. Cisplatin solution was administered at doses of 5, 10 and 20 mg/kg, respectively. Cisplatin-loaded nanoparticles were administered as a saline solution at the equivalent cisplatin doses of 5, 10 and 20 mg/kg. For i.p. injections, similar experiments were conducted except that the equivalent cisplatin doses were 5 or 10 mg/kg, respectively.

All mice were tagged, and tumors were measured every other day with calipers during the period of study. The tumor volume was calculated by the formula $(W^2 \times L)/2$, where W is the tumor measurement at the widest point, and L is the tumor dimension at the longest point. Each animal was weighed at the time of treatment so that dosages could be adjusted to achieve the mg/kg amounts reported. Animals also were weighed every other day throughout the experiments.

2.8. FDG–PET/CT imaging

Mice that received intratumoral cisplatin-loaded nanoparticles (5 mg/kg), free cisplatin (5 mg/kg) and saline were selected for PET/CT imaging on Day 7. The mice were kept in the anesthetized condition during the whole PET/CT scanning procedure. Fasting for 4 h or more before tracer injection is necessary because elevation of blood sugar reduces tissue FDG uptake by competitive inhibition and lowers the sensitivity of tumor detection. 14.8 MBq (400 μCi) of ^{18}F-FDG was injected via the tail vein as a radiotracer for imaging and detection of an increased rate of aerobic glycolysis. The imaging studies were performed with a combined PET/CT scanner for clinical use (Jemini JXL, Philips, USA). High resolution PET images were acquired with the mice 45 min after the administration of ^{18}F-FDG, and the same field of view was covered as for CT. PET images were corrected for attenuation and scatter on the basis of the CT data. The image fusion was performed by an automatic image fusion system, using vendor-supplied software. Maximum FDG uptake values in the tumor were obtained for the standard uptake value (SUV) calculations, applying corrections for body weight and injected activity. SUVs provide a normalized quantitative measure of tissue FDG accumulation by normalizing the tissue radioactivity measured with PET to the injected dose and the body weight of the mice.

3. Results and discussion

3.1. Fabrication and characterization of mPEG–PCL nanoparticles

3.1.1. Polymer synthesis, size distribution and zeta potential detection

mPEG–PCL block copolymers were prepared by ring opening polymerization of ε-caprolactone in the presence of mPEG with a small amount of stannous octoate as catalyst. The copolymers with different chemical compositions were prepared by changing the molar ratio of PEG/CL monomer and the molecular weight of PEG. The molecular weight of the polymers was obtained from ^{1}H NMR and GPC as showed from our previous reports [19,22]. The feed ratio and calculated molecular weight from NMR are summarized in Table 1. The molecular weight and molecular weight distribution of the two samples from GPC also are listed in Table 1.

Fig. 1 shows the TEM and AFM micrograph of a batch of typical polymeric nanoparticles (mPEG4k–PCL20k). TEM image clearly shows the nearly spherical shape of the polymeric nanoparticles with minor deformation. AFM micrograph with higher magnifications confirms the spherical shape of nanoparticles with a smooth surface.

Table 1
Major characteristics of the synthesized mPEG–PCL block copolymer

Copolymers	PEG M_n	M_n[a]	M_n[b]	M_w[b]	Pd[b]
PCL20k–PEG4k	4000	26,800	18,600	30,480	1.64
PCL30k–PEG10k	10,000	42,300	31,980	49,300	1.54

Pd, polydispersity, defined as the ratio of weight-average molecular weight to the number-average molecular weight (M_w/M_n).
[a] Determined by ^{1}H NMR.
[b] Determined by GPC.

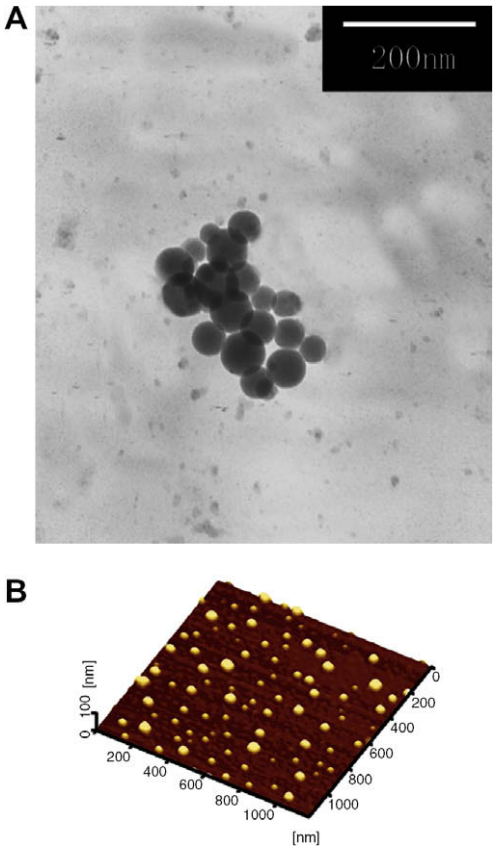

Fig. 1. (A) TEM image of mPEG–PCL nanoparticles (mPEG4k–PCL20k). (B) AFM image of mPEG–PCL nanoparticles (mPEG4k–PCL20k).

The particle size and zeta potential of the nanoparticles is measured by DLS (Table 2). The mean diameter of mPEG4k–PCL20k is around 70 nm, while mPEG10k–PCL30k has a larger diameter of about 90 nm. Both the two nanoparticles exhibit a negative zeta potential slightly below 0 mV. (Table 2) As is reported in previous research, polyester nanoparticles without PEG surface coating display a more negative zeta potential around −35 mV, while PEG outer shell is capable to screen the surface charge in certain degree [23–25].

3.1.2. Determination of drug loading and encapsulation efficiency

Table 2 shows the drug loading content and encapsulation efficiency of the two nanoparticles. The yield of both nanoparticles is higher than 90%, indicating no important loss of materials during the preparation process. By varying the feeding ratio of copolymer and cisplatin, the highest drug loading content of cisplatin into mPEG4k–PCL20k nanoparticles was detected as 5.28 ± 0.73%. As for mPEG10k–PCL30k nanoparticles, the highest drug loading content was 3.13 ± 0.45%. Both of them do have high encapsulation efficiency of more than 75%. This was due to the utilization of chloride ions during the preparation process. Though cisplatin has low water solubility, the soluble part of cisplatin can dissociate and release chloride in water, whereas this dissociation is inhibited by the presence of chloride ions [26]. Earlier studies about the encapsulation of cisplatin into nanoparticles formed by PDEA–PEG or PLGA–PEG reported a drug loading content varying from 0.1% to 5% [4,10,11,27]. Thus, the cisplatin-loaded nanoparticles formed in the current research posses a satisfying drug loading content and encapsulation efficiency. In the following in vitro and in vivo evaluation, we applied the cisplatin-loaded nanoparticles formed by mPEG4k–PCL20k because of its relatively higher DLE and EE.

3.2. In vitro release of cisplatin-loaded nanoparticles

Fig. 2 shows the cisplatin release profile of cisplatin-loaded mPEG4k–PCL20k nanoparticles. An initial burst of more than 30% release in 5 h indicates that a certain amount of cisplatin was on the surface of the nanoparticles. In the following period, release of cisplatin was observed in a sustained manner from the core–shell nanoparticles as shown in Fig. 2. Actually, 3 days incubation with PBS caused a total 60% higher release. In contrast, the release profile of free cisplatin solution in PBS reveals a total release of more than 80% in the first 2 h (Fig. 2). These data indicated that cisplatin can be released from the core–shell structure of polymeric nanoparticles and the cisplatin-loaded nanoparticles might be useful as a controlled release system for this anticancer drug.

3.3. In vitro cytotoxicity of cisplatin-loaded nanoparticles

In the first test for BGC823 cells, the empty nanoparticle caused a less than 20% cell death even when its concentration reached 1000 μg/ml (data not shown). Both cisplatin and cisplatin-loaded nanoparticles displayed resembling concentration and time-dependent cytotoxicity (Fig. 3A). In detail, a 24 h incubation of cisplatin or cisplatin-loaded nanoparticles alone resulted in a less than 40% cell growth inhibition even at a maximum concentration of 8 μg/ml. Extending the incubation time to 48 h of two samples, respectively, led to a noticeable lower cell viability at each dose compared with that of 24 h. Both cisplatin and cisplatin-loaded nanoparticles substantially suppressed the growth of more than 80% of total cells at the highest dose of 8 μg/ml. Moreover, the percentage of cell viability further declined when another 24 h incubation time was allowed on the basis of 48 h incubation. The calculated IC_{50} values of cisplatin-loaded nanoparticles were a little higher than those of free cisplatin during different times. It meant that cisplatin-loaded nanoparticles showed lower cytotoxic-

Table 2
Mean particle size and drug load efficiency of two kinds of nanoparticles

Nanoparticles	Particle size[a] (nm)	Polydispersity	Zeta potential (mV)	DLC[b] (%)	EE[c] (%)	Yield (%)
PCL20k–PEG4k	71.3 ± 0.4	0.13 ± 0.03	−5.4 ± 1.2	5.28 ± 0.73	88.3 ± 9.3	93 ± 2.7
PCL30k–PEG10k	90.1 ± 1.2	0.14 ± 0.06	−8.4 ± 2.3	3.13 ± 0.45	79.4 ± 7.5	90 ± 3.1

[a] The SD value was for the mean particle size obtained from the three measurements of a single batch.
[b] DLC, drug loading content.
[c] EE, encapsulation efficiency.

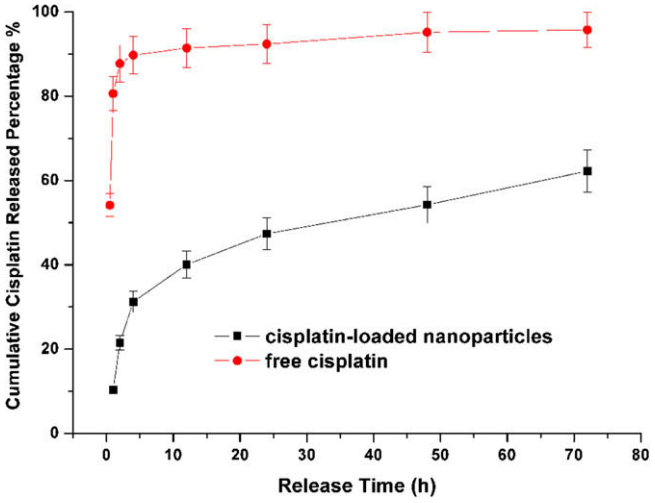

Fig. 2. Cumulative in vitro release profile of cisplatin from mPEG–PCL nanoparticles.

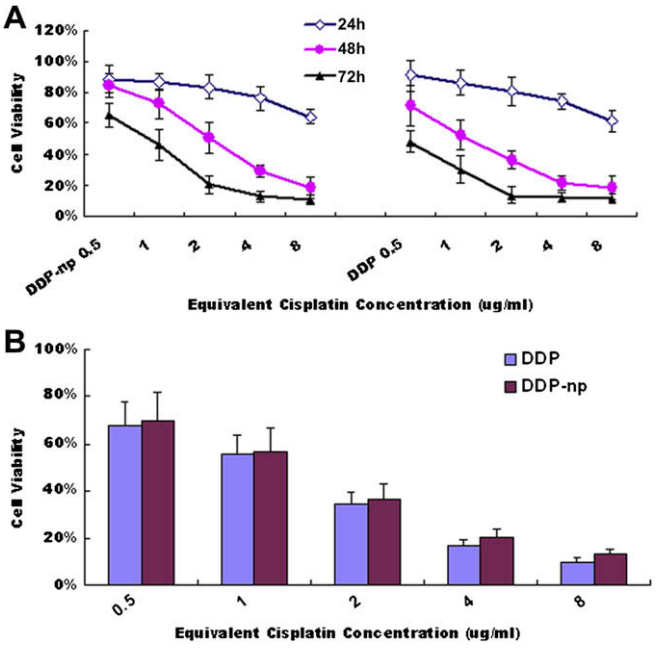

Fig. 3. Cytotoxicity of cisplatin-loaded nanoparticles on different kinds of cancer cell lines. (A) Time-dependent inhibition profiles of free cisplatin (DDP) and cisplatin-loaded nanoparticles (DDP-np) against BGC823 cells. (B) Cytotoxicity of free cisplatin and cisplatin-loaded nanoparticles against H_{22} cells for 48 h. Data are presented as mean ± SD (n = 3).

ity than free cisplatin at an equivalent dose, which is in accordance with other reports [9,10,27,28]. Reasonable explanation could be deduced from the core–shell structure of the nanoparticles. The sustained release of the drug-loaded nanoparticles determines that certain time is required to release the drug into the culture medium. When incubated with the cells, the drug concentration of cisplatin-loaded nanoparticles slowly increased due to its sustained release profile.

In another cytotoxicity test, H_{22} cells were exposed to the same doses of cisplatin and cisplatin-loaded nanoparticles for 48 h as in BGC823 assay. (Fig. 3B) The obtained results confirmed the trend found in the test of BGC823 cells. Cisplatin expressed similar cytotoxicity than cisplatin-loaded nanoparticles.

3.4. In vivo antitumor effect of cisplatin-loaded nanoparticles

Tumor nodules formed by subcutaneous engraftment of H_{22} cell line were treated with the drug-loaded nanoparticles at various doses on the basis of cisplatin. To explore the most optimum delivery of cisplatin-loaded nanoparticles, two administration routes (i.t., i.p.) were adopted to better compare the antitumor efficiency between free cisplatin and its polymeric formulation. Intratumoral delivery was applied as the preferable administration route due to its substantial high drug concentration in tumor and characteristic pharmacokinetics. In comparison, intraperitoneal administration was selected as a pathway for systemic delivery of cisplatin.

Fig. 4A depicted the changes of tumor volume by i.t. administration in H_{22} tumor-bearing mice. Both free cisplatin and cisplatin-loaded nanoparticles effectively inhibited tumor growth and displayed a dose-dependent antitumor efficacy, while no antitumor effect was observed in the group of empty nanoparticles. The difference of tumor volume between the group of cisplatin-loaded nanoparticles and saline was highly significant ($p < 0.01$), as was the difference between the group of free cisplatin and saline ($p < 0.01$) as determined by the two-tailed t test. Tumor volumes in groups receiving saline and empty nanoparticles increased rapidly from Day 7 with their mean volumes reaching more than 5000 mm^3 on Day 13. In comparison, groups receiving cisplatin-loaded nanoparticles and free cisplatin showed a retarded tumor growth with their mean volumes less than 2000 mm^3 on Day 13.

Most importantly, cisplatin-loaded nanoparticles exhibited more efficient antitumor efficacy than free cisplatin by delaying tumor growth. Growth of tumor nodules in the groups receiving cisplatin-loaded nanoparticles remained almost invisible with their mean volumes no more than 800 mm^3 at the end of therapy. In contrast, tumor nodules for the groups receiving three doses of free cisplatin grew a little faster with their mean volumes more than 1200 mm^3 at the termination of the experiment. Statistic analysis revealed that the group receiving each dose of cisplatin-loaded nanoparticles (5, 10, 20 mg/kg) had significantly smaller tumors when compared to the group receiving the corresponding dose of free cisplatin ($p < 0.05$) from Day 9 to Day 13.

The efficacy of cisplatin-loaded nanoparticles also was evaluated in the same animal model via i.p. administration as a standard regimen for drug delivery (Fig. 5A). The preliminary experiment indicated that i.p. administration of 20 mg/kg of cisplatin cause death in mice. Thus, in the current study, the doses of cisplatin-loaded nanoparticles were adjusted to 5 and 10 mg/kg on a cisplatin basis, as was equal to the low and medium doses of the i.t. experiment. As shown in Fig. 5A, cisplatin-loaded nanoparticles

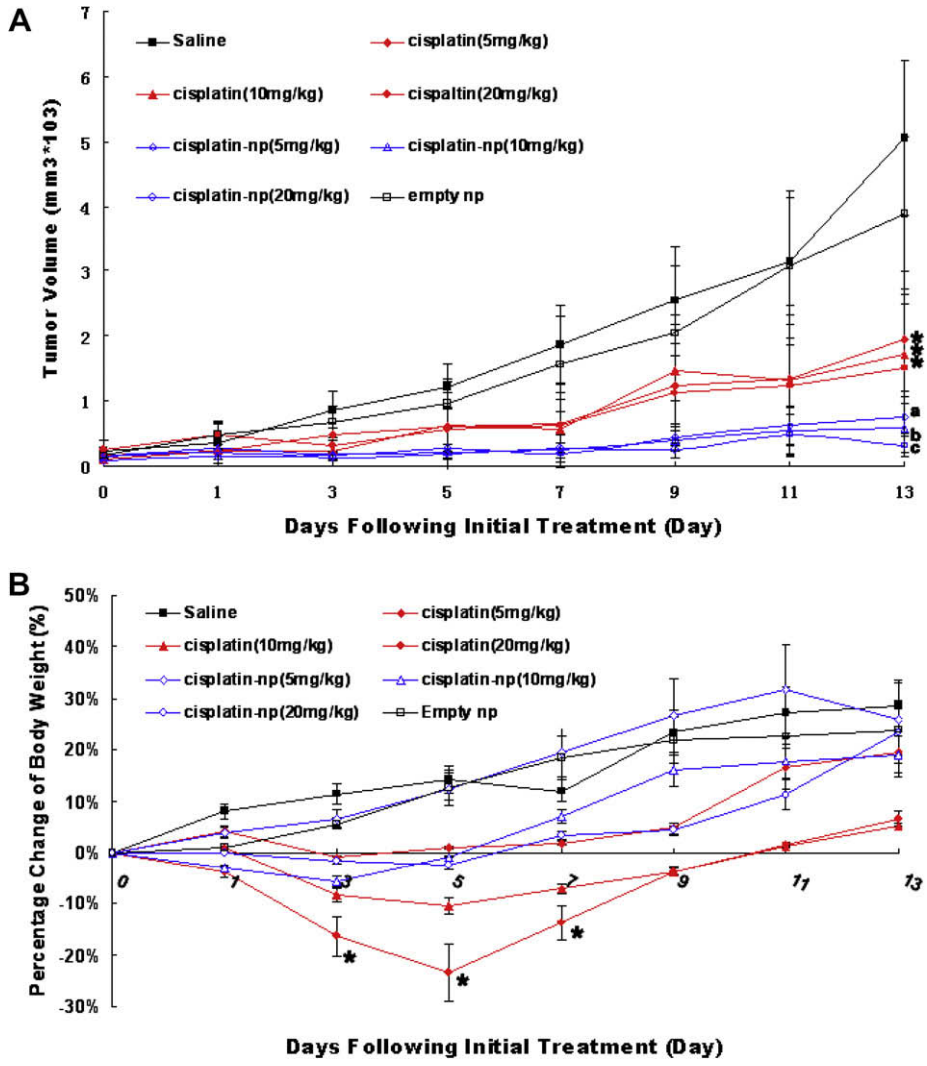

Fig. 4. (A) Tumor volume of established H_{22} xenografts in ICR mice during therapy under different treatments. Mice were treated with different protocols on Day 0 (arrow) as showed in the figure. Saline: vehicle; empty np: empty nanoparticles; DDP: free cisplatin at a dose of 5, 10 and 20 mg/kg, respectively; DDP-np: cisplatin-loaded nanoparticles in a saline solution at equivalent cisplatin doses of 5, 10 and 20 mg/kg, respectively. Different agents were delivered through intratumoral pathway when tumor volume measured 100 mm^3. Data are presented as mean ± SD ($n = 6$). The difference between tumor volumes in the group of saline and cisplatin-loaded nanoparticles is highly significant ($p < 0.01$). Significant difference ($p < 0.05$) also is observed between the group of free cisplatin and cisplatin-loaded nanoparticles at the equivalent dose. * represents $p < 0.05$ versus the saline group. a represents $p < 0.05$ versus the group receiving 5 mg/kg free cisplatin. [b] represents $p < 0.05$ versus the group receiving 10 mg/kg free cisplatin. [c] represents $p < 0.05$ versus the group receiving 20 mg/kg free cisplatin. (B) Bodyweight change of ICR mice receiving different treatments during therapy. * represents $p < 0.05$ versus the saline group. Data are presented as mean ± SD ($n = 6$).

at 5 and 10 mg/kg both produced significant reduction in growth rate when compared to saline group ($p < 0.05$). Additionally, free cisplatin also proved to be efficacious (versus saline group, $p < 0.05$) as tumors appeared to be slightly larger than in the groups receiving the corresponding doses of cisplatin-loaded nanoparticles. Among the four therapeutic groups, cisplatin-loaded nanoparticles at a dose of 10 mg/kg produced the greatest tumor growth reduction, while cisplatin at 5 mg/kg generated a relatively minimal reduction in growth rate. However, no significant differences in tumor volumes were observed between cisplatin groups and the groups receiving cisplatin-loaded nanoparticles at the same dose throughout the whole evaluation.

An analysis of body weight variations generally defined the adverse effects of the different therapy regiments. For i.t. administration, cisplatin-loaded nanoparticles demonstrated favorable results without any obvious body weight loss even at the highest dose, whereas free cisplatin induced severe weight loss (Fig. 4B). For instance, body weight in the group receiving 20 mg/kg free cisplatin manifested a remarkable loss of more than 20% of the original weight on Day 7 ($p < 0.01$ versus control). On the same day, the cisplatin group at 10 mg/kg also showed a nearly 10% body weight loss ($p < 0.05$ versus control). Moreover, the mice receiving free cisplatin were in a weak state in aspects of movement, spirit and skin luster, while no obvious alteration was observed in nanoparticle-treated animals. On the contrary, Fig. 5B revealed that compared to the saline group, the mice in the groups receiving free cisplatin and cisplatin-loaded nanoparticles at 10 mg/kg demonstrated a slight decrease in bodyweight in the first 5 days. These results partially indicated that cisplatin-loaded nanoparticles generated less toxicities than free cisplatin when administered intratumorally.

A literature search in the database revealed that there are several studies explored the in vivo efficacy of cisplatin [4,9,29–31]. Xu et al. examined the antitumor effect of cisplatin-loaded nanoparticles through i.p. administration. The drug-loaded nanoparticles formed by mPEG–PCL showed no advantage over free cisplatin in ovarian tumor models [4]. Other studies from Kataoka et al. and Ye et al. proved the enhanced efficiency of cisplatin–polymer conjugates through a systemic (i.v.) delivery [9,29]. Fujiia et al.

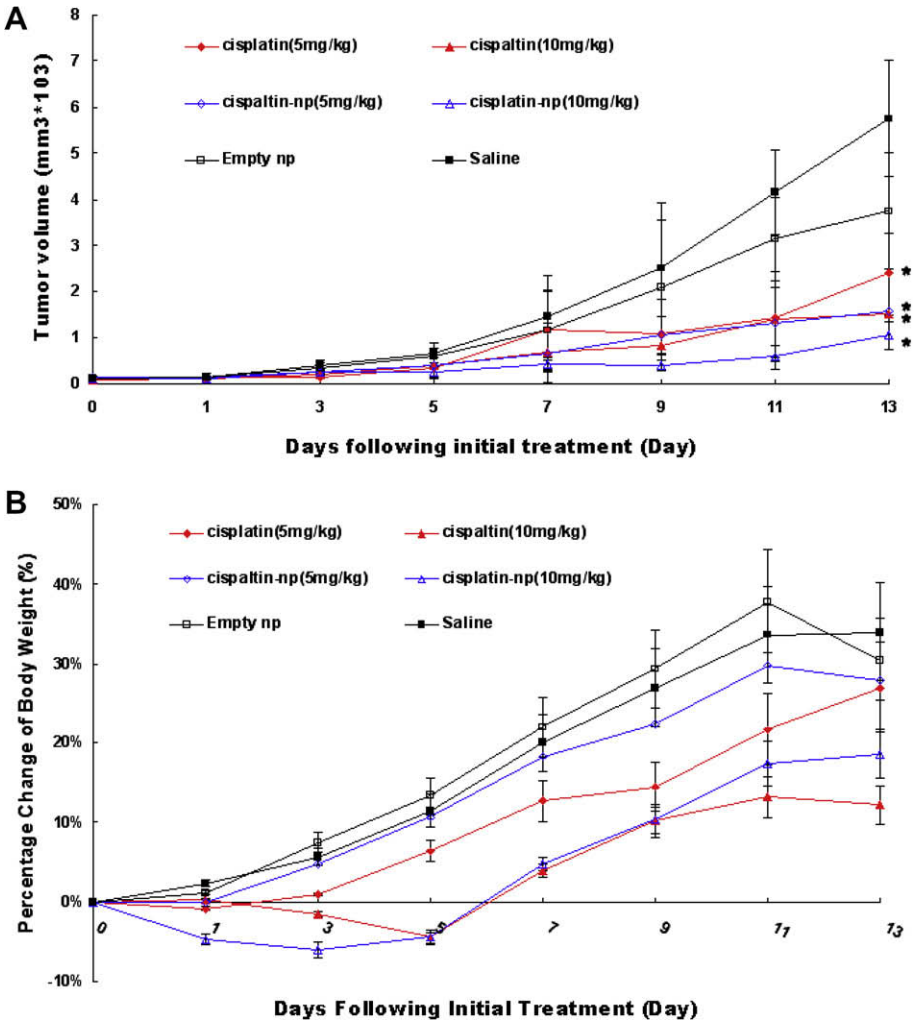

Fig. 5. (A) Tumor volume of established H_{22} xenografts in ICR mice during therapy under different treatments. Mice were treated with different protocols on Day 0 (arrow) as shown in the figure. Saline: vehicle; empty np: empty nanoparticles; DDP: free cisplatin at a dose of 5 and 10 mg/kg; DDP-np: cisplatin-loaded nanoparticles in a saline solution at equivalent cisplatin doses of 5 and 10 mg/kg. Different agents were delivered through intraperitoneal pathway when tumor volume measured 100 mm^3. * represents $p < 0.05$ versus the saline group. Data are presented as mean ± SD ($n = 6$). The difference between tumor volumes in the group of saline and cisplatin-loaded nanoparticles is highly significant ($p < 0.01$). No significant difference also is observed between the group of free cisplatin and cisplatin-loaded nanoparticles at the equivalent dose. (B) Bodyweight change of ICR mice receiving different treatments during therapy. Data are presented as mean ± SD ($n = 6$).

investigated the in vivo efficacy of cisplatin incorporated gelatin hydrogel through a local administration. Significant improvement was observed in the antitumor efficacy of cisplatin incorporated gelatin hydrogel compared with free cisplatin [30,31]. However, the local delivery was achieved by an operation. Cisplatin–hydrogel must be implanted under the tumor mass after making a transverse skin incision.

In the in vivo experiments reported here, we compared the in vivo efficacy of cisplatin-loaded nanoparticles to equivalent dosing with free cisplatin that was given locally as an i.t. injection or systemically i.p. injection. As shown in the results, cisplatin-loaded nanoparticles with a local delivery toward tumor site were more efficient in impeding tumor development than free cisplatin, whereas the nanoparticles demonstrated no superior efficacy to free cisplatin by the systemic administration. Similar results were observed from the studies of Xu et al. that systemic administration of cisplatin-loaded nanoparticles could not enhance the anticancer efficacy of cisplatin [4].

The enhanced efficiency of intratumoral delivery against intraperitoneal administration may be related to the characteristic pharmacodynamics and pharmacokinetics profile. Intratumoral administration is regarded as a site-specific delivery to tumor nodule, which will accordingly induce a higher local drug concentration than systemic delivery [13]. Besides, the relatively lower drug concentration in plasma by local delivery, compared to systemic administration, means the less toxicity to normal tissues.

Possible mechanisms underlying the superiority of cisplatin-loaded nanoparticles against free cisplatin delivered intratumorally may include the continuous exposure of tumor mass to released cisplatin from the nanoparticles. Though cisplatin-loaded nanoparticles by i.t. administration cannot achieve as high initial concentration as free cisplatin, the sustained release of cisplatin is capable to deliver its antitumor efficacy constantly. It has been reported that antitumor activity of cisplatin depends on the dose and exposure time [32]. Evidence of treatment of efficacy between cisplatin and its controlled delivery system also were obtained from the study of Fujii et al. [30]. Detection of cisplatin concentration of both free cisplatin and cisplatin–hydrogel when injected intratumorally showed that the drug concentration of cisplatin–hydrogel in tumor site become increasingly higher than that of free cisplatin with time going on. Consequently, significant difference in tumor growth and survival rates could be observed between these two groups [30]. However, the following reasons may be responsible for the absence of significant difference in tumor growth between

the two groups receiving cisplatin-loaded nanoparticles and free cisplatin delivered intraperitoneally. First, deficiency in the specificity to the tumor makes it difficult for chemotherapeutics by systemic administration (i.v. or i.p.) to expect the high therapeutic efficacy. Second, the rapid clearance of released cisplatin from the nanoparticles injected intraperitoneally prevents further tumor-eliminating efficiency brought by the drug. On the contrary, a slower elimination rate in the tumor site is expected due to the impaired lymphatic system of tumor issue [33]. As a result, it is highly reasonable that released cisplatin from the intratumorally delivered nanoparticles retain in the interstitial space of the tumor for a longer time compared to normal tissue and exerts protracted tumor-eliminating effect locally.

3.5. PET/CT imaging

Representative examples of CT, PET and fusion images of the three groups are displayed in Fig. 6. Coronal images from CT clearly indicated that transplanted tumors were noticeable in the left side of the thorax of the mice receiving saline or free cisplatin, whereas the established tumors in the mice receiving cisplatin-loaded nanoparticles were almost invisible (Fig. 6). FDG–PET revealed that increased FDG uptake was readily observed in the tumor of the mouse receiving saline or free cisplatin and CT confirmed that this focal tracer uptake corresponded to the tumor area. Conversely, no obvious FDG uptake was detected by PET in the nanoparticle-treated mice (Fig. 6).

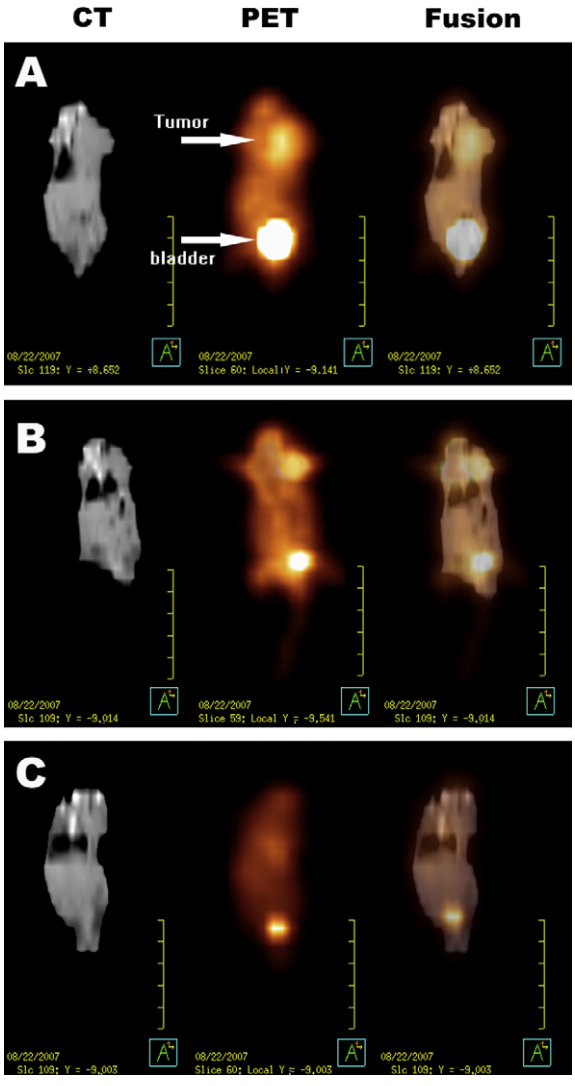

Fig. 6. Male ICR mice bearing a subcutaneous H_{22} (murine hepatoma cell line) tumor at the left side of the thorax. CT, PET and fused PET/CT images are arranged in the figure from left to right. (A) Coronal images of a mouse in the control group (saline). (B) Coronal images of a mouse in the group receiving intratumoral free cisplatin (5 mg/kg). (C) Coronal images of a mouse in the group receiving intratumoral cisplatin-loaded nanoparticles (5 mg/kg).

Hence, ^{18}F-FDG accumulation signified the decreased glucose utilization in the tumor site of the mice receiving cisplatin-loaded nanoparticles. Calculation by the software showed an average SUV of 0.87 ± 0.13, which was significantly lower than that of the other two groups ($p < 0.01$). In comparison, the mice in the control group experienced a higher glucose uptake with a mean SUV reaching 3.12 ± 0.47. Similar results were obtained in the mice receiving free cisplatin with an average SUV of 3.48 ± 0.39. There was no significant difference in SUV between the groups receiving saline and free cisplatin ($p > 0.05$).

CT scanning confirmed the enhanced efficiency of i.t. delivered cisplatin-loaded nanoparticles by showing the decreased tumor volume. Furthermore, evidence of the treatment efficacy between cisplatin-loaded nanoparticles and free cisplatin also was obtained from the PET images as an indicator for glucose utilization. The lowest FDG uptake of the tumor in nanoparticle-treated mice means the poorest tumor metabolism rate, thereby indicating the slowest tumor growth in this group.

The results obtained from PET/CT directly displayed the treatment response of different therapy regimens and offered a novel way to evaluate the efficiency of nanoparticle based therapies. Employment of PET/CT in oncological studies makes it more accurate and fast to measure treatment response by assessing tumor metabolic changes instead of variations in tumor size. Glucose uptake (SUV) detected before and during treatment present quantitative assessment, thus predicting response to treatment in various tumors [34,35]. Moreover, FDG–PET/CT provided additional information about the extent of the disease, the metabolic activity within tumor metastases, and the response to therapy following initiation of therapy. Therefore, the information from PET/CT imaging would be of great interest for validation of evaluation of treatment response. Meanwhile, this study demonstrated that small animal imaging with a clinical PET/CT scanner is quite feasible and adequate for non-invasive imaging in evaluating the antitumor efficiency of drug-loaded nanoparticles.

Planned modifications of the core–shell structure nanoparticles utilized in this study are under active consideration as a part of this ongoing research. Further development in optimizing the therapeutic regimen on the basis of i.t. administration will be fully reviewed in human xenograft models in order to further expand the parameters of this current research. Further study in the author's laboratory is conducted to seek the optimal conditions for applying PET/CT in animal experiments. In addition, previous reports from the author's laboratory showed that, in combination with hyperthermia, enhanced antitumor efficacy of a metastable docetaxel-loaded polymeric micelle whose size is around 80 nm is observed on the basis of EPR effect [36,37]. Thus, together with the current findings, it is of great value in future experiments to focus on the combinational antitumor effect of hyperthermia and local delivery of thermosensitive micelles.

4. Conclusions

This study reported a spherical core–shell structure nanoparticle formed by amphilic mPEG–PCL block copolymers. Cisplatin was incorporated into the nanoparticles with high encapsulation efficiency. In vitro studies using BGC823 and Lovo cell lines proved the cytotoxicity of cisplatin-loaded nanoparticles in a dose and

time-dependent manner. In vivo evaluation and PET/CT imaging have demonstrated for the first time that cisplatin-loaded nanoparticles, when delivered intratumorally, exhibited significantly increased antitumor efficacy, and, moreover, substantially decreased the tumor metabolism rate in comparison to free cisplatin in an established H_{22} transplanted mice model. It is concluded that intratumoral delivery of the drug-loaded nanoparticles is the most promising method in countering the spread of tumors, and continuing research will definitely advance this study. It is fully understood and appreciated that the development of local chemotherapy with nanoscale drug formation warrants more intensive research in order to further characterize the detailed mechanism in the uptake of drug-loaded nanoparticles the interaction between drug release and tumors, and, ultimately, the feasibility and advantages of clinical applications.

Acknowledgements

This work was supported by the National Natural Science Foundation of China (No. 30670958), Jiangsu Province Key Medical Cent Foundation and Scientific and Technological Innovation Plan Fund of Postgraduate from Jiangsu Province.

References

[1] T. Hogberg, B. Glimelius, P. Nygren, SBU-group. Swedish Council of Technology Assessment in Health Care, a systematic overview of chemotherapy effects in ovarian cancer, Acta Oncol. 40 (2001) 340–360.
[2] S.A. Hundahl, Surgical quality in trials of adjuvant cancer therapy, J. Surg. Oncol. 80 (2002) 177–180.
[3] X. Yao, K. Panichpisal, N. Kurtzman, K. Nugent, Cisplatin nephrotoxicity: a review, Am. J. Med. Sci. 334 (2007) 115–124.
[4] P. Xu, E.A. Van Kirk, W.J. Murdoch, Y. Zhan, D.D. Isaak, M. Radosz, Y. Shen, Anticancer efficacies of cisplatin-releasing pH-responsive nanoparticles, Biomacromolecules 7 (2006) 829–835.
[5] H. Sasaki, S. Niimi, M. Akiyama, T. Tanaka, A. Hazato, S. Kurozumi, S. Fukusima, M. Fusushima, Antitumor activity of 13,14-dihydro-15-deoxy-D7-prostaglandin-A1-methyl ester integrated into lipid microspheres against human ovarian cancer cells resistant to cisplatin in vivo, Cancer Res. 59 (1999) 3919–3922.
[6] H. Araki, T. Tani, M. Kodama, Anti-tumor effect of cisplatin incorporated into polylactic acid microcapsules, Artif. Organs 23 (1999) 161–168.
[7] N. Nishiyama, K. Kataoka, Preparation and characterization of size-controlled polymeric micelle containing cis-dichlorodiammineplatinum(II) in the core, J. Control. Release 74 (2001) 83–94.
[8] M. Yokoyama, T. Okano, Y. Sakurai, S. Suwa, K. Kataoka, Introduction of cisplatin into polymeric micelle, J. Control. Release 39 (1996) 351–356.
[9] N. Nishiyama, S. Okazaki, H. Cabral, M. Miyamoto, Y. Kato, Y. Sugiyama, K. Nishio, Y. Matsumura, K. Kataoka, Novel cisplatin-incorporated polymeric micelles can eradicate solid tumors in mice, Cancer Res. 63 (2003) 8977–8983.
[10] E.C. Gryparis, M. Hatziapostolou, E. Papadimitriou, K. Avgoustakis, Anticancer activity of cisplatin-loaded PLGA–mPEG nanoparticles on LNCaP prostate cancer cells, Eur. J. Pharm. Biopharm. 67 (2007) 1–8.
[11] K. Avgoustakis, A. Beletsi, Z. Panagi, P. Klepetsanis, A.G. Karydas, D.S. Ithakissios, PLGA–mPEG nanoparticles of cisplatin: in vitro nanoparticle degradation, in vitro drug release and in vivo drug residence in blood properties, J. Control. Release 79 (2002) 123–135.
[12] H. Idani, J. Matsuoka, T. Yasuda, K. Kobayashi, N. Tanaka, Intra-tumoral injection of doxorubicin (Adriamycin) encapsulated in liposome inhibits tumor growth, prolongs survival time and is not associated with local or systemic side effects, Int. J. Cancer 88 (2000) 645–651.
[13] K.A. Walter, R.J. Tamargo, A. Olivi, P.C. Burger, H. Brem, Intratumoral chemotherapy, Neurosurgery 37 (1995) 1128–1145.
[14] S. Ning, N. Yu, D.M. Brown, S. Kanekal, S.J. Knox, Radiosensitization by intratumoral administration of cisplatin in a sustained-release drug delivery system, Radiother. Oncol. 50 (1999) 215–223.
[15] E. Harper, W. Dang, R.G. Lapidus, R.I. Garver Jr., Enhanced efficacy of a novel controlled release paclitaxel formulation (PACLIMER Delivery System) for local-regional therapy of lung cancer tumor nodules in mice, Clin. Cancer Res. 5 (1999) 4242–4248.
[16] M. Tatsumi, Y. Nakamoto, B. Traughber, L.T. Marshall, J.F.H. Geschwind, R.L. Wahll, Initial experience in small animal tumor imaging with a clinical positron emission tomography/computed tomography scanner using 2-[F-18]fluoro-2-deoxy-D-glucose, Cancer Res. 63 (2003) 6252–6257.
[17] K.E. Uhrich, S.M. Cannizzaro, R.S. Langer, K.M. Shakesheff, Polymeric systems for controlled drug release, Chem. Rev. 99 (1999) 3181–3198.
[18] D.A. Herold, K. Keil, D.E. Bruns, Oxidation of polyethylene glycol by alcohol dehydrogenase, Biochem. Pharmacol. 38 (1989) 73–76.
[19] Y. Hu, J. Xie, Y. Tong, C. Wang, Effect of PEG conformation and particle size on the cellular uptake efficiency of nanoparticles with the HepG2 cells, J. Control. Release 118 (2007) 7–17.
[20] I. Maziekien, L. Ermanis, T.J. Walsh, Assay procedure for platinum in reforming catalysis, Anal. Chem. 32 (1960) 645–647.
[21] T. Mosmann, Rapid colorimetric assay for cellular growth and survival: application to proliferation and cytotoxicity assay, J. Immunol. Methods 65 (1983) 55–63.
[22] Y. Hu, X. Jiang, Y. Ding, L. Zhang, C. Yang, J. Zhang, J. Chen, Y. Yang, Preparation and drug release behaviors of nimodipine-loaded poly(caprolactone)–poly(ethylene oxide)–polylactide amphiphilic copolymer nanoparticles, Biomaterials 24 (2003) 2395–2404.
[23] L. Zhang, M. Yang, Q. Wang, Y. Li, R. Guo, X. Jiang, C. Yang, B. Liu, 10-Hydroxycamptothecin loaded nanoparticles: Preparation and antitumor activity in mice, J. Control. Release 119 (2007) 153–162.
[24] L. Zhang, Y. Hu, X. Jiang, C. Yang, W. Lu, Y. Yang, Camptothecin derivative-loaded poly(caprolactone-co-lactide)-b–PEG–b-poly(caprolactone-co-lactide) nanoparticles and their biodistribution in mice, J. Control. Release 96 (2004) 135–148.
[25] A.E. Hawley, L. Illum, S.S. Davis, Preparation of biodegradable, surface engineered PLGA nanospheres with enhanced lymphatic drainage and lymph node uptake, Pharm. Res. 14 (5) (1997) 657–661.
[26] B.W. Wenclawiak, M. Wollmann, Separation of platinum(II) anti-tumour drugs by micellar electrokinetic capillary chromatography, J. Chromatogr. A 724 (1996) 317–326.
[27] P. Xu, E.A. Van Kirk, S. Li, W.J. Murdoch, J. Zhen, M.D. Hassain, M. Radosz, Y. Shen, Highly stable core-surface-crosslinked nanoparticles as cisplatin carriers for cancer chemotherapy, Colloids Surf. B Biointerfaces 48 (2006) 50–57.
[28] X.L. Yan, R.A. Gemeinhart, Cisplatin delivery from poly(acrylic acid-co-methyl methacrylate) microparticles, J. Control. Release 106 (1–2) (2005) 198–208.
[29] H. Ye, L. Jin, R. Hu, Z. Yi, J. Li, Y. Wu, X. Xi, Z. Wu, Poly(g,l-glutamic acid)–cisplatin conjugate effectively inhibits human breast tumor xenografted in nude mice, Biomaterials 27 (2006) 5958–5965.
[30] M. Konishi, Y. Tabata, M. Kariya, A. Suziki, M. Mandai, K. Nanbu, K. Takakura, S. Fujii, In vivo anti-tumor effect through the controlled release of cisplatin from biodegradable gelatin hydrogel, J. Control. Release 92 (2003) 301–313.
[31] M. Konishi, Y. Tabata, M. Kariya, H. Hosseinkhani, A. Suziki, K. Fukuhara, M. Mandai, K. Takakura, S. Fujii, In vivo anti-tumor effect of dual release of cisplatin and adriamycin from biodegradable gelatin hydrogel, J. Control. Release 103 (2005) 7–19.
[32] N. Kurihara, T. Kubota, Y. Hoshiya, Y. Otani, M. Watanabe, K. Kumai, M. Kitajima, Antitumor activity of cis-diamminedichloroplatinum (II) against human tumor xenografts depends on its area under the curve in nude mice, J. Surg. Oncol. 61 (1996) 138–142.
[33] Y. Noguchi, J. Wu, R. Duncan, J. Steohalm, K. Ulbrich, T. Akaike, H. Maeda, Early phase tumor accumulation of macromolecules: a great difference in clearance rate between tumor and normal tissues, Jpn. J. Cancer Res. 89 (1998) 307–314.
[34] G.J. Kelloff, J.M. Hoffman, B. Johnson, H.I. Scher, B.A. Siegel, E.Y. Cheng, B.D. Cheson, J. O'shaughnessy, K.Z. Guyton, D.A. Mankoff, L. Shankar, S.M. Larson, C.C. Sigman, R.L. Schilsky, D.C. Sullivan, Progress and promise of FDG–PET imaging for cancer patient management and oncologic drug development, Clin. Cancer Res. 11 (2005) 2785–2808.
[35] W.A. Weber, Use of PET for monitoring cancer therapy and for predicting outcome, J. Nucl. Med. 46 (2005) 983–995.
[36] M. Yang, Y. Ding, L. Zhang, X. Qian, X. Jiang, B. Liu, Novel thermosensitive polymeric micelles for docetaxel delivery, J. Biomed. Mater. Res. A 81 (2007) 847–857.
[37] B. Liu, M. Yang, X. Li, X. Qian, Z. Shen, Y. Ding, L. Yu, Enhanced efficiency of thermally targeted taxanes delivery in a human xenograft model of gastric cancer, J. Pharm. Sci. doi:10.1002/jps.21194.